scientific reports

Check for updates

OPEN

Genome edited intestine liver on a chip system for integrated intestinal hepatic drug absorption and metabolism evaluation

Ryosuke Negoro[1]✉, Sayaka Deguchi[2], Daiju Yamazaki[3], Kazuo Takayama[2] & Takuya Fujita[1]

Evaluation of the intestinal absorption and hepatic metabolism is crucial to the development of orally administered drugs. Previous evaluation systems have assessed intestinal epithelial cells and hepatocytes separately. To develop an experimental system that accounts for drug transfer from the intestine to the liver, we generated a genome-edited intestine-liver-on-a-chip system (genome-edited chip) by incorporating high drug metabolism capacity genome-edited Caco-2 cells in the top channel and CYPs-UGT1A1 KI-HepG2 cells in the bottom channel of a polydimethylsiloxane-based microfluidic device. We demonstrated that the genome-edited chip enables simultaneous evaluation of drug absorption and metabolism by allowing sample collection from both the top and bottom channels. We then confirmed the feasibility of the system in experiments showing that the concentrations of CYP3A4 metabolites decreased under the influence of itraconazole or bergamottin, known CYP3A4 inhibitors. These results validate the utility of the genome-edited chip as a convenient and cost-effective tool for drug absorption and metabolism experiments that takes into account the influence of both the small intestine and liver. This system represents a significant advancement in pharmacokinetic evaluation, offering a more integrated approach to understanding drug behavior in the body. By mimicking the sequential process of intestinal absorption followed by hepatic metabolism, the genome-edited chip provides a more physiologically relevant model compared to traditional single-cell type systems.

Keywords Organs-on-a-chip, Drug absorption, Drug-metabolizing enzyme, Caco-2 cells, HepG2 cells

Abbreviations

CYPs-UGT1A1 KI-HepG2 cells	CYP3A4-POR-UGT1A1-CYP1A2-CYP2C19-CYP2C9-CYP2D6 knock-in-HepG2 cells
Genome-edited Caco-2 cells	CYP3A4-POR-UGT1A1-CES2 knock-in and CES1 knock-out Caco-2 cells
MPS	Microphysiological systems
PDMS	Polydimethylsiloxane
PDMS device	PDMS-based microfluidic device
PHHs	Primary human hepatocytes

Orally administered drugs are absorbed through the small intestine and reach the liver via the portal vein, where they undergo metabolism before entering systemic circulation. Therefore, the absorption and metabolism of drugs in the small intestine, as well as their metabolism in the liver, are critical factors in predicting the pharmacokinetics of orally administered drugs. In nonclinical studies, human colon carcinoma-derived Caco-2 cells and primary human hepatocytes (PHHs) are widely used to evaluate pharmacokinetics in the small intestine and liver. However, these models present several challenges. Caco-2 cells express only low levels of key drug-metabolizing enzymes, such as cytochrome P450 (CYP) 3A4[1–4]. PHHs, while useful for evaluating drug metabolism and hepatotoxicity, have significant lot-to-lot variability and high cost[5,6]. Human hepatoblastoma cell line-derived HepG2 cells offer a more affordable and reproducible alternative. However, they have a major

[1]Laboratory of Molecular Pharmacokinetics, College of Pharmaceutical Sciences, Ritsumeikan University, 1-1-1 Noji-Higashi, Kusatsu 525-8577, Japan. [2]Department of Synthetic Human Body System, Medical Research Institute, Institute of Integrated Research, Institute of Science Tokyo, 1-5-45 Yushima, Bunkyo-ku, Tokyo 113-8510, Japan. [3]Division of Pharmacology, Center for Biological Safety and Research, National Institute of Health Sciences, 3–25–26 Tono-machi, Kawasaki-ku, Kawasaki 210–9501, Japan. ✉email: negoro-r@fc.ritsumei.ac.jp

limitation in that they express very low levels of several important drug-metabolizing enzymes[7,8]. Additionally, there are challenges with current experimental methods. In small intestine models, only Caco-2 cells are used to predict intestinal absorption rates, while in liver models, PHHs are employed to assess hepatic metabolism and hepatotoxicity. These isolated approaches do not adequately replicate the continuous drug transfer from the gut to the liver that occurs in vivo. Consequently, predicting pharmacokinetics in a physiologically relevant manner is challenging, and current experiments cannot fully mimic the gut-to-liver drug transfer observed in living organisms.

Evaluation using experimental animals such as mice has been conducted, but accurate pharmacokinetic assessment has been hindered by the species differences between experimental animals and humans[9,10]. To address this issue, evaluation systems using human liver chimeric mice have been developed. While these mice have improved the predictability of hepatic metabolism and hepatotoxicity, concerns persist in the use of this model for evaluating the pharmacokinetics of orally administered drugs due to the mouse-derived small intestine[11,12]. Moreover, human liver chimeric mice are difficult to produce in large numbers, are expensive, and raise ethical concerns.

We have employed genome-editing technologies to create CYP3A4-P450 oxidoreductase (POR)-UDP glucuronosyltransferase family 1 member A1 (UGT1A1)-carboxylesterase 2 (CES2) knock-in (KI) and carboxylesterase 1 (CES1) knock-out (KO) Caco-2 (genome-edited Caco-2) cells and CYP3A4–POR–UGT1A1–CYP1A2–CYP2C19–CYP2C9–CYP2D6 (CYPs–UGT1A1) KI-HepG2 cells to improve in vitro intestinal epithelial and hepatocyte models[13–15]. These enhanced models address some limitations of conventional Caco-2 and HepG2 cells and have demonstrated the ability to assess drug metabolism. In particular, the drug-metabolizing capacity of CYP1A2, 2C9, 2C19, 2D6, and 3A4 in CYP-UGT1A1 KI-HepG2 cells was comparable to that of PHHs cultured for 48 hr[14,15]. However, despite these advancements, we have not yet developed an experimental system that replicates the continuous drug transfer from the gut to the liver as observed in living organisms. In other words, while progress has been made in refining individual cellular models, an integrated approach that mimics the dynamic process of gut-to-liver drug transfer in vivo remains to be realized. Recently, microphysiological systems (MPS), which utilize microfluidic devices to replicate biological organ interactions in vitro, have garnered significant attention[16,17]. Several studies have demonstrated the application of MPS in pharmacokinetic research by combining intestinal epithelial and hepatocyte models on microfluidic devices[18–22]. However, the range of drugs evaluated in these studies remains limited, and the full potential of MPS for pharmacokinetic prediction has yet to be fully explored.

In this study, we attempted to construct a pharmacokinetic evaluation system that mimics continuous drug transfer from the intestine to the liver by mounting genome-edited Caco-2 cells and CYPs-UGT1A1 KI-HepG2 cells with high drug metabolism capacity on a microfluidic device. We then investigated whether pharmacokinetic evaluation considering a series of processes from intestinal absorption to hepatic metabolism was feasible using this evaluation system.

Materials and methods

Cell culture

Parental HepG2 cells (RGB1648) and Caco-2 cells (RGB0988) were provided by RIKEN BRC through the National Bio-Resource Project of the MEXT/AMED, Japan. The HepG2 cells and Caco-2 cells were cultured with Dulbecco's Modified Eagle Medium (DMEM; Nacalai Tesque) containing 10% fetal bovine serum (FBS; Sigma-Aldrich), 1% MEM Non-Essential Amino Acids Solution (Nacalai Tesque) and 1% Antibiotic–Antimycotic Mixed Stock Solution (Nacalai Tesque).

Fabrication of PDMS-based microfluidic devices

The fabrication of a polydimethylsiloxane (PDMS)-based microfluidic device (PDMS device) was described previously[23]. The microfluidic device consists of two layers of microchannels separated by single or two-polyethylene terephthalate (PET) membranes containing 3.0 μm pores (Cat# 353091; Corning). The single-PET membrane PDMS device was used for drug permeability assay. Two-PET membrane PDMS devices were used to isolate Caco-2 and HepG2 cells and to analyze their gene expression levels by real-time RT-PCR.

Intestine-liver-on-a-chip

Before seeding Caco-2 cells, the top channel of the PDMS device was pre-coated with 1.6 μg/cm^2 fibronectin (Cat# F0895; Sigma-Aldrich). Caco-2 cells were suspended at 1×10^7 cells/mL in DMEM containing 10% FBS, 1% MEM Non-Essential Amino Acids Solution and 1% Antibiotic–Antimycotic Mixed Stock Solution (hereafter referred to as Medium). Ten microliters (1×10^5 cells) of suspension medium was injected into the fibronectin-coated top channel. Then, the device was incubated for 1 h. After the incubation, the top and bottom channels of the PDMS device were each filled with 200 μl of Medium.

Ten days later, HepG2 cells were seeded into the bottom channel as follows. First, the bottom channel of the PDMS device was pre-coated with 1.6 μg/cm^2 Collagen I solution (Cat# ASC-1–100-20; Nippi). The HepG2 cells were then suspended at 1×10^7 cells/mL in Medium, and 10 μL (1×10^5 cells) of the suspension medium was injected into the Collagen I-coated bottom channel. Then, the device was turned upside down and incubated for 1 h. After the incubation, the device was turned over, and the top and bottom channel of the PDMS device were each filled with 200 μl of Medium.

Four days later (14 days after Caco-2 cell seeding), the PDMS devices cultured with Caco-2 and HepG2 cells were used as the intestine-liver-on-a-chip system for various experiments. The intestine-liver-on-a-chip was maintained with a change of Medium in both channels every 2 days.

Real-time RT-PCR

The total RNA isolated, cDNA synthesized and real-time RT-PCR protocol was described previously[4,13,14]. We used the human adult small intestine total RNA (BioChain) and 48-h cultured primary human hepatocytes (PHHs 48 h) as a positive control. The Real-time RT-PCR primer sequences are summarized in Supplemental Information (Table S1).

Immunocytochemistry

The immunocytochemistry protocol was described previously[4]. Primary antibody used were anti-human Zo-1 antibody conjugated to Alexa Fluor 488 (Cat# 339188; Thermo Fisher Scientific), Anti-Villin antibody (Cat#ab130751; abcam), E-cadherin Polyclonal antibody (Cat# 20874–1-AP; Proteintech), CYP1A2 antibody (Cat#sc-53241; Santa Cruz Biotechnology), CYP2C8/9/18/19 Polyclonal antibody (Cat# 16546–1-AP; Proteintech), CYP2D6/7 Polyclonal antibody (Cat# 17868–1-AP; Proteintech) or CYP3A4 antibody (Cat#sc-53850; Santa Cruz Biotechnology). Secondary antibody used were Goat anti-Rabbit IgG (Heavy Chain), Superclonal™ Recombinant Secondary Antibody, Alexa Fluor™ 488 (Cat# A27034; Thermo Fisher Scientific), Donkey anti-Mouse IgG (H + L) Highly Cross-Adsorbed Secondary AntibodyAlexa Fluor™ Plus 594 (Cat# A32744; Thermo Fisher Scientific) or Donkey anti-Rabbit IgG (H + L) Highly Cross-Adsorbed Secondary Antibody, Alexa Fluor™ Plus 594 (Cat# A32754; Thermo Fisher Scientific).

Live/dead staining

The intestine-liver-on-a-chip was washed with pH 7.4 Hanks' Balanced Salt Solution (HBSS). The chip was then exposed to a solution containing 1 µM Calcein-AM (Nacalai Tesque) and 1 µg/ml 7-Aminoactinomycin D (7-AAD; Nacalai Tesque) in pH 7.4 HBSS and incubated in a CO_2 incubator for 30 min for staining. Following this, the chip was washed with pH 7.4 HBSS and observed using BZ-X710 (Keyence).

Lucifer yellow permeability assay

Transport buffer [pH 7.4 Hank's Balanced Salt Solution (HBSS; Sigma-Aldrich) containing 10 mM HEPES and 25 mM glucose] containing 100 µM Lucifer Yellow CH (LY; Nacalai Tesque) was added to the top channel, and the intestine-liver-on-a-chip was incubated at 37℃ for 120 min. The samples were collected from the bottom channel. The top and bottom channels of the PDMS device were filled with 300 µL and 200 µL of transport buffer medium, respectively. LY fluorescent signals were measured with an SH-9500 Lab microplate reader (Corona Electric) using 428 nm excitation and 536 nm emission. The analysis of apparent membrane permeability (*Papp*) was conducted as described previously[4].

Drug permeability assay

After 13 days of culture, the top channel of the intestine-liver-on-a-chip was treated with Medium in the presence or absence of either of the CYP3A4 inhibitors, 10 µM itraconazole (Tokyo Chemical Industry) or 10 µM bergamottin (Sigma-Aldrich), for the remainder of the 14-day culture period. After 14 days of culture, Medium containing 10 µM acetaminophen (APAP; Tokyo Chemical Industry), 10 µM caffeine (Nacalai Tesque), 10 µM triazolam (FUJIFILM Wako Pure Chemical Corporation) (metabolite: α-hydroxy triazolam; Sigma-Aldrich), 10 µM diclofenac (Tokyo Chemical Industry) (metabolite: 4'-hydroxy diclofenac; Cayman Chemical), 1 µM bufuralol (Cayman Chemical) (metabolite: 1'-hydroxy bufuralol; Cayman Chemical) or 1 µM propranolol (FUJIFILM Wako Pure Chemical Corporation) (metabolite: desisopropylpropranolol; Toronto Research Chemicals) was added to the top channel. The intestine-liver-on-a-chip was incubated at 37 °C, and 50 µL samples were collected from the top and bottom channels after 2, 4, 24, and 48 h of incubation. The top and bottom channels were topped off with 50 µL of Medium immediately after sampling. The Infinity Rocker Pro (Next Advance) was set to 0.1 cycle/min, and dynamic perfusion was applied only during drug permeability assays. The samples were collected from the supernatant, then immediately mixed with an equal volume of acetonitrile. The mixed solutions were centrifuged for 5 min at 15,000 g. The samples were filtered with a Cosmonice Filter W with 0.45 µm pore size (Nacalai Tesque), then analyzed by LC–MS/MS. LC–MS/MS was performed using a LCMS-8060NX (Shimadzu). Using the automatic multiple-reaction monitoring (MRM) optimization function, we adjusted the MS/MS settings for each component to obtain the optimal response for quantifying each drug (Figure S1). Detailed information for the ionization mode and MRM transition of the mass spectrometer is summarized in Table S2. The dwell time for each MRM transition was set at 100 ms. LC separations were performed at 40 °C with COSMOCORE(R) 2.6C18 Packed Column 2.1 mm I.D. × 50 mm (Cat#12631-41; Nacalai Tesque). The mobile phase condition is summarized in Table S3.

Measurement of drug absorption into the PDMS device and 96 well plate

The PDMS device or 96 well plate (Cat# 655180; Greiner Bio-one) were cultured with Medium containing 10 µM acetaminophen, 10 µM caffeine, 10 µM triazolam, 10 µM diclofenac, 1 µM bufuralol or 1 µM propranolol. The amount of Medium in the PDMS device and PS plate is 200 µL/channel and 200 µL/well, respectively. The PDMS device or 96 well plate were incubated at 37 °C, and 50 µL samples were collected from the top channels or 96 well plate at 2, 4, 24, and 48 h time points. The top channels were topped up with 50 µL of Medium immediately after sampling. The samples were collected from the supernatant, then immediately mixed with same volume of acetonitrile. The mixed solutions were centrifuged for 5 min at 15,000 g. The samples were filtered with a Cosmonice Filter W with 0.45 µm pore size, then analyzed by LC–MS/MS. LC–MS/MS was performed using a LCMS-8060NX (Shimadzu).

Statistical analysis

Statistical analyses were done as indicated in figure legends using Easy R (EZR) software. A value of $p < 0.05$ was considered statistically significant.

Results

Characterization of the intestine-liver-on-a-chip

To generate the intestine-liver-on-a-chip, either wild-type (WT)-Caco-2 cells or genome-edited Caco-2 cells were seeded in the top channel of the PDMS device and cultured for 10 days. Subsequently, either WT-HepG2 cells or CYPs-UGT1A1 KI-HepG2 cells were seeded into the bottom channel and cultured for an additional 4 days (Fig. 1A). Two variants of the intestine-liver-on-a-chip model were established: (1) the WT intestine-liver-on-a-chip (WT chip), co-cultured with WT-Caco-2 and WT-HepG2 cells, and (2) the genome-edited intestine-liver-on-a-chip (genome-edited chip), co-cultured with genome-edited Caco-2 and CYPs-UGT1A1 KI HepG2 cells. These two chip models were used throughout the study to compare the effects of genetic modifications on drug metabolism in the intestine–liver axis. First, we analyzed gene expression levels in the intestine-liver-on-a-chip during the co-culture of Caco-2 and HepG2 cells. The analysis focused on four categories of markers: (1) intestinal markers [*villin 1 (VIL1), sucrase-isomaltase (SI), and intestine-specific homeobox (ISX)*], (2) hepatocyte markers [*albumin (ALB), asialoglycoprotein receptor 1 (ASGR1) and hepatocyte nuclear factor 4 alpha (HNF4A)*], (3) drug-metabolizing enzymes [*cytochrome P450 3A4 (CYP3A4), carboxylesterase 1 (CES1), carboxylesterase 2 (CES2) P450 oxidoreductase (POR), UDP glucuronosyltransferase family 1 member A1 (UGT1A1), cytochrome P450 family 1 subfamily A member 2 (CYP1A2), cytochrome P450 family 2 subfamily C member 9 (CYP2C9), cytochrome P450 family 2 subfamily C member 19 (CYP2C19), cytochrome P450 family 2 subfamily D member 6 (CYP2D6)*] and (4) drug transporters [*ATP-binding cassette subfamily B member 1 (ABCB1), ATP-binding cassette subfamily G member 2 (ABCG2), solute carrier family 15 member 1 (SLC15A1)*]. The gene expression levels were quantified using real-time RT-PCR. The gene expression levels of intestinal markers, drug-metabolizing enzymes (*CYP3A4, CES1, CES2, POR, UGT1A1*), and drug transporters showed no significant differences between the co-culture of genome-edited Caco-2 and CYPs-UGT1A1 KI-HepG2 cells and their mono-culture counterparts (Fig. 1B). A similar pattern was observed for hepatocyte markers and drug-metabolizing enzymes (*CYP1A2, CYP2C9, CYP2C19, CYP2D6, CYP3A4, POR, UGT1A1*) in CYPs-UGT1A1 KI-HepG2 cells (Fig. 1C). Likewise, the gene expression levels in the co-culture of WT-Caco-2 and WT-HepG2 cells were comparable to those in their mono-cultures (Fig. S1A). This trend persisted for WT-HepG2 cells, with no significant differences in the expression of hepatocyte markers and drug-metabolizing enzymes between co-cultures and mono-cultures (Fig. S1B).

Next, to characterize Caco-2 and HepG2 cells in the intestine-liver-on-a-chip, immunostaining was performed for the tight junction marker zonula occludens-1 (Zo-1), VIL1, intercellular junction marker E-cadherin, CYP1A2, CYP2C9/19, CYP2D6 and CYP3A4 (Figs. 2A, S2A and S2B). In both the WT and genome-edited chips, Caco-2 cells displayed positive staining for Zo-1, VIL1, and E-cadherin. CYP1A2, CYP2C9/19, CYP2D6, and CYP3A4 in the CYPs-UGT1A1 KI-HepG2 cells were strongly stained compared to WT-HepG2 cells, consistent with the gene expression results. The WT-HepG2 cells and CYPs-UGT1A1 KI-HepG2 cells in the intestine-liver-on-a-chip exhibited an aggregate morphology, so Live-Dead staining was performed using Calcein-AM to stain live cells and 7-AAD to stain dead cells (Fig. S2C). The WT-HepG2 cells and CYPs-UGT1A1 KI-HepG2 cells were predominantly stained with Calcein-AM, indicating that they were viable.

In addition, the barrier functions of the WT and genome-edited chip monolayers were analyzed by LY permeability assay (Fig. 2B). The *Papp* of LY was below 1.0×10^{-6} cm/s, indicating that the intestine-liver-on-a-chip successfully formed sufficient monolayers. Notably, the *Papp* of LY was lower in both the WT and genome-edited chips compared to the *Papp* observed in WT or genome-edited Caco-2 cells mono-culture. These results suggest that Caco-2 and HepG2 cells can be co-cultured on PDMS devices with minimal negative impact, successfully forming intact monolayers.

Drug absorption and metabolism experiments using intestine-liver-on-a-chip

We next evaluated whether the intestine-liver-on-a-chip could be used to simultaneously assess drug absorption and metabolism. To conduct drug absorption and metabolism experiments under dynamic perfusion conditions, the Infinity Rocker Pro was set to 0.1 cycle/min, and this condition was designated as the Flow group. Dynamic perfusion was applied only during the drug absorption and metabolism experiments. The group that underwent experiments under static conditions was designated as the Static group.

APAP and caffeine were chosen as model drugs [oral bioavailability (F) > 0.7] with minimal first-pass effects[24]. Triazolam, diclofenac, bufuralol, and propranolol were employed to evaluate the utility of the intestine-liver-on-a-chip for assessing drug metabolism. Initially, due to the potential for significant drug concentration fluctuations caused by sorption in the PDMS devices[23,25,26], sorption experiments were conducted for all six drugs used in this study (Fig. S3). Additionally, 96-well plates made of polystyrene were used as positive controls. APAP, caffeine, and diclofenac exhibited negligible sorption to PDMS. In contrast, non-negligible sorption was observed for triazolam, bufuralol, and propranolol.

APAP, caffeine, triazolam, diclofenac, bufuralol and propranolol were administered to the apical channel of the intestine-liver-on-a-chip. Drug concentrations were then monitored over time in both the apical and bottom channels.

Under static conditions, the concentrations of APAP and caffeine remained constant in the top channel in both WT and genome-edited chips (Fig. 3A,B). However, the concentrations in the bottom channel increased in a time-dependent manner in both chip types (Fig. 3A,B). Under flow conditions, the concentrations of APAP and caffeine decreased compared to the initial concentration of 10 μM at 24 and 48 h in both the WT and genome-edited chips. Consistent with the decrease in APAP and caffeine concentrations in the top channel, the

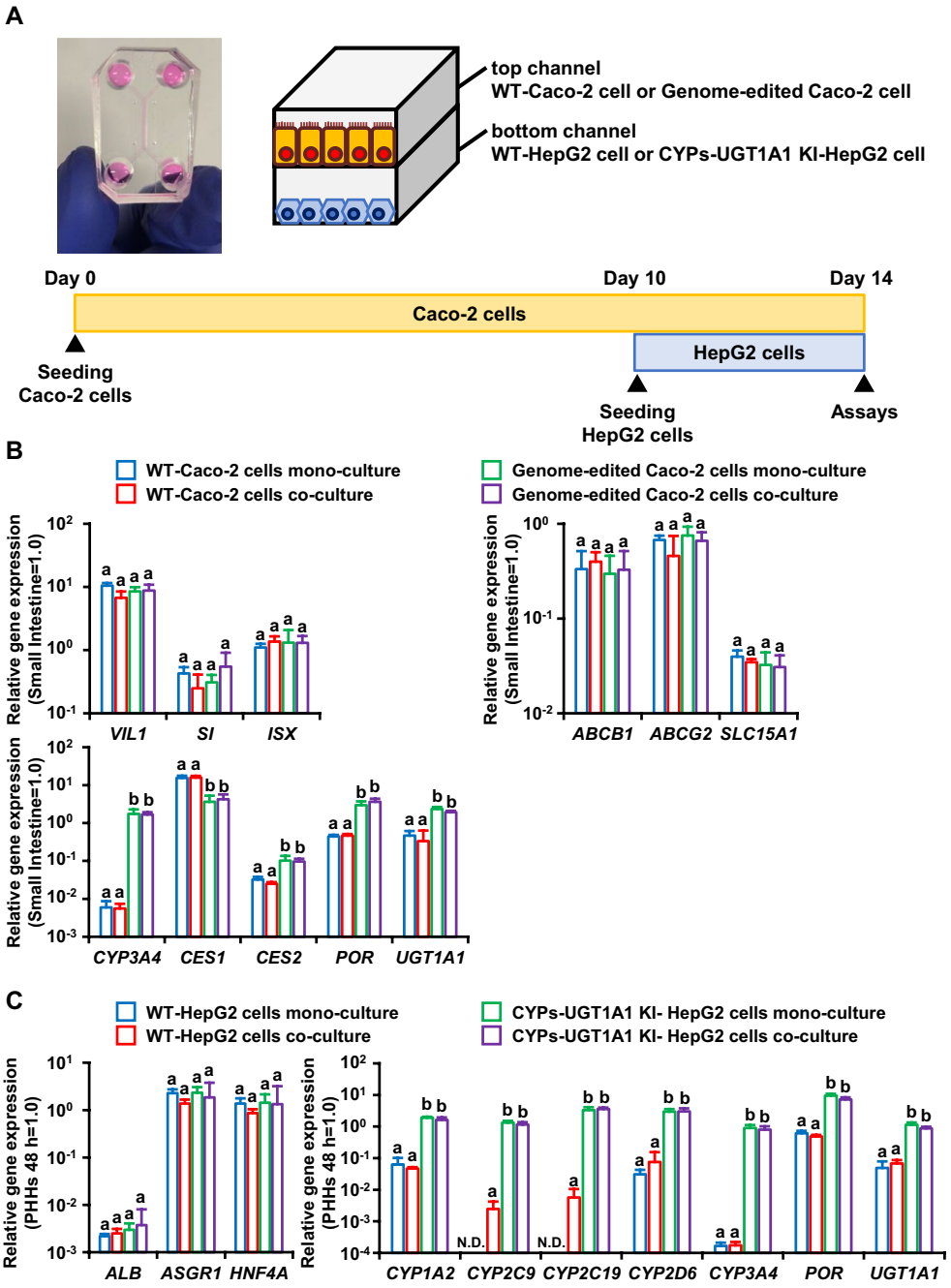

Fig. 1. Gene expression analysis of the genome-edited intestine-liver-on-a-chip. (**A**) Schematic of the intestine-liver-on-a-chip. (**B**) The gene expression levels of intestinal epithelial cell markers (*VIL1, SI, ISX*), drug transporters (*ABCB1*, *ABCG2*, *SLC15A1*) and drug-metabolizing enzymes (*CYP3A4*, *CES1*, *CES2*, *POR*, *UGT1A1*) were examined in WT-Caco-2 cells mono-culture, co-culture with WT-HepG2 cells, genome-edited Caco-2 cells mono-culture and co-culture with CYPs-UGT1A1 KI-HepG2 cells by real-time RT-PCR. On the y axis, the gene expression levels in the human small intestine were taken as 1.0. (**C**) The gene expression levels of hepatic markers (*ALB*, *ASGR1*, *HNF4A*) and drug-metabolizing enzymes (*CYP1A2*, *CYP2C9*, *CYP2C19*, *CYP2D6*, *CYP3A4*, *POR*, *UGT1A1*) in WT-HepG2 cells mono-culture, co-culture with WT-Caco-2 cells, CYPs-UGT1A1 KI-HepG2 cells mono-culture and co-culture with genome-edited Caco-2 cells. On the y axis, the gene expression levels in the PHHs at 48 h were taken as 1.0. Data represent the means ± SDs ($n = 3$ devices). Statistical significance was evaluated by oneway ANOVA followed by Tukey's post hoc test ($p < 0.05$). Groups that do not share the same letter had significantly different results.

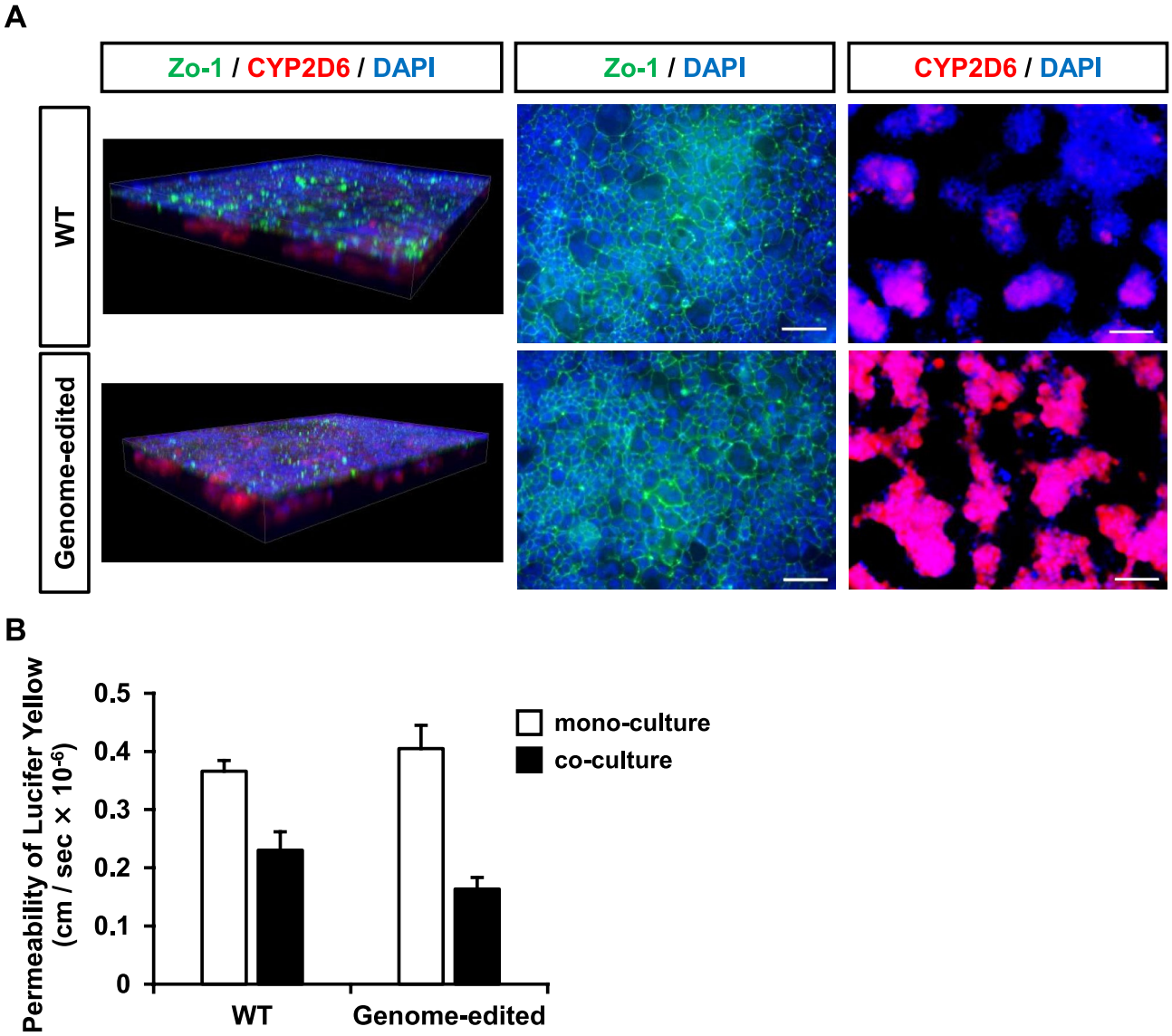

Fig. 2. Characterization of the intestine-liver-on-a-chip. (**A**) Immunostaining analysis of Zo-1 (green) and CYP2D6 (red) was performed in the WT and genome-edited intestine-liver-on-a-chip. Nuclei were stained with DAPI (blue). Scale bars represent 100 μm. (**B**) Apical-to-basolateral permeability of 100 μM LY across the intestine-liver-on-a- intestine-liver-on-a-chip was measured. Data represent the means ± SDs ($n = 3$ devices).

concentrations of APAP and caffeine in the bottom channel increased substantially at 24 h in both chip types (Fig. 3A,B). Notably, under flow conditions, the APAP concentrations in the top channel of the genome-edited chip at 24 and 48 h were slightly higher than those in the WT chip.

Triazolam, a drug metabolized by CYP3A4, showed a rapid decrease in concentration in the top channel of both the WT and genome-edited chips within 4 h of administration under both static and flow conditions (Fig. 3C). The concentration of triazolam in the bottom channel increased substantially under flow conditions. Additionally, the triazolam concentrations in genome-edited chips under flow conditions were lower than those in WT chips at 24 and 48 h (Fig. 3C).

The concentration of diclofenac, a drug metabolized by CYP2C9, in the top channel under static and flow conditions was slightly reduced compared to the initial concentration of 10 μM in both WT and genome-edited chips (Fig. 3D). Under flow conditions, the diclofenac concentration in the bottom channel increased substantially compared to static conditions, but there was no significant difference between WT and genome-edited chips (Fig. 3D).

Bufuralol, a drug metabolized by CYP2D6, showed a rapid decrease in concentration in the top channel 2 h after administration in both the WT and genome-edited chips, followed by a time-dependent decline under both static and flow conditions (Fig. 3E). Under flow conditions, the concentration of bufuralol in the bottom channel increased substantially compared to static conditions (Fig. 3E). Furthermore, after 48 h, the bufuralol concentration was slightly lower in the genome-edited chips than in the WT chips.

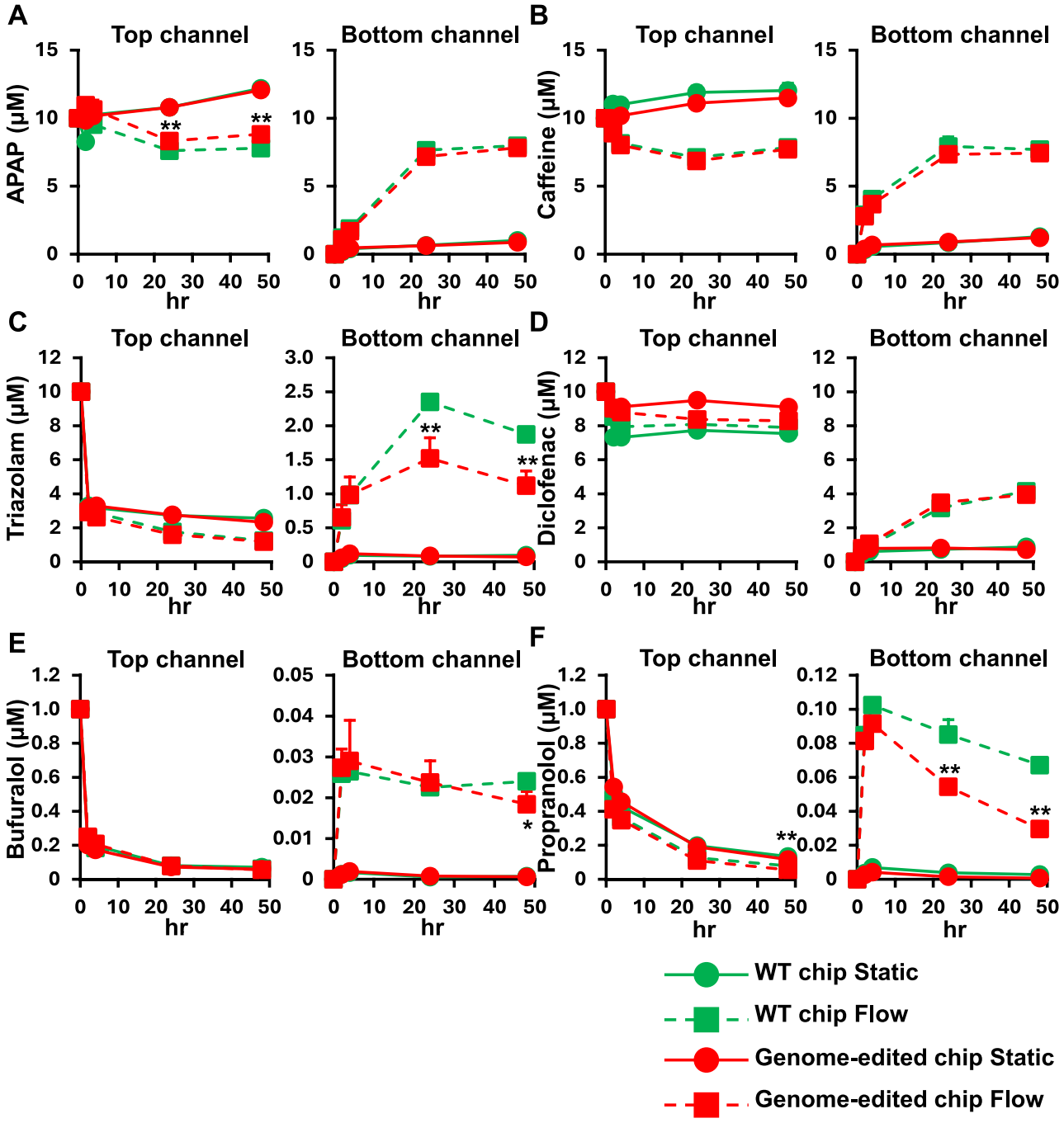

Fig. 3. Drug permeability assay using the intestine-liver-on-a-chip. Apical-to-basolateral permeability of 10 μM acetaminophen (**A**), 10 μM caffeine (**B**), 10 μM triazolam (**C**), 10 μM diclofenac (**D**), 1 μM bufuralol (**E**) and 1 μM propranolol (**F**) across the WT and genome-edited intestine-liver-on-a-chip. The statistical significance of differences in the drug concentrations between the WT chip Flow and genome-edited chip Flow at the same time points (24 h and 48 h) was determined using Student's *t*-test (*$p < 0.05$, **$p < 0.01$). Data represent the means ± SDs ($n = 4$ devices).

Propranolol is a drug metabolized by CYP2D6, CYP1A2, and other enzymes. Under both static and flow conditions, its concentration in the top channel rapidly decreased in both WT and genome-edited chips within 2–4 h after administration, followed by a time-dependent decline (Fig. 3F). Under flow conditions, propranolol concentrations in the bottom channel increased substantially (Fig. 3F). At 24 and 48 h, the concentrations in the genome-edited chips were significantly lower than those in the WT chips.

Next, metabolite concentrations of triazolam, diclofenac, bufuralol, and propranolol in the intestine-liver-on-a-chip were evaluated. α-Hydroxy triazolam (α-OH triazolam), a CYP3A4 metabolite of triazolam, showed a time-dependent increase in concentration in both the top and bottom channels of the genome-edited chip

under both static and flow conditions (Fig. 4A). Furthermore, under flow conditions, the concentration of α-OH triazolam in the genome-edited chip increased substantially and was higher than that observed in the WT chip (Fig. 4A).

The concentration of 4-hydroxy diclofenac (4-OH diclofenac), a CYP2C9 metabolite of diclofenac, increased in a time-dependent manner in both the top and bottom channels of the genome-edited chip under both static and flow conditions (Fig. 4B). The concentration of 4-OH diclofenac in the top and botom channel at 24 and 48 h was higher in the genome-edited chip Flow compared to the WT chip Flow (Fig. 4B). Interestingly, the concentration of 4-OH diclofenac in the top channel of the genome-edited chip under static conditions was higher than that under flow conditions.

1-Hydroxy bufuralol (1-OH bufuralol), a CYP2D6 metabolite of bufuralol, showed a time-dependent increase in concentration in both the top and bottom channels of the genome-edited chip under both static and flow conditions (Fig. 4C). Under flow conditions, 1-OH bufuralol concentrations in both the top and bottom channels at 24 and 48 h were higher in the genome-edited chip compared to the WT chip (Fig. 4C). Furthermore, under flow conditions, the concentration of 1-OH bufuralol in the genome-edited chip increased substantially and was higher than that observed in the static conditions.

The concentration of desisopropylpropranolol (ISOPRO), a CYP1A2 metabolite of propranolol, in both the top and bottom channels was higher in the genome-edited chip under flow conditions compared to the WT chip

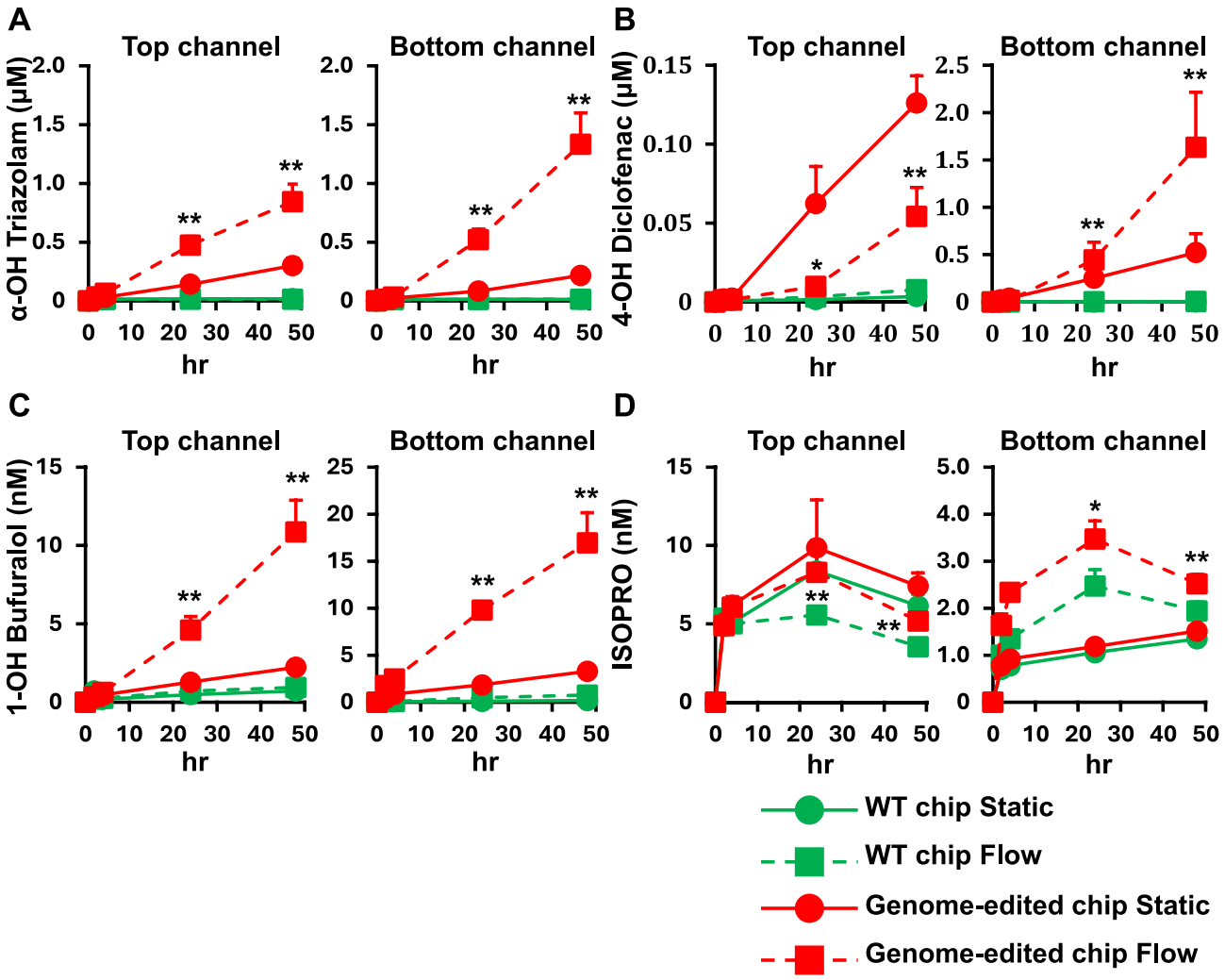

Fig. 4. Evaluation of the drug-metabolizing activity of the intestine-liver-on-a-chip. (**A**) The CYP3A4 activities in the WT and genome-edited chip were examined by quantifying the metabolites of α-OH triazolam. (**B**) The CYP2C9 activities in the WT and genome-edited intestine-liver-on-a-chip were examined by quantifying the metabolites of 4-OH diclofenac. (**C**) The CYP2D6 activities in the WT and genome-edited intestine-liver-on-a-chip were examined by quantifying the metabolites of 1-OH bufuralol. (**D**) The CYP1A2 activities in the WT and genome-edited intestine-liver-on-a-chip were examined by quantifying the metabolites of ISOPRO. The statistical significance of differences in drug concentrations between the WT chip Flow and genome-edited chip Flow at the same time points (24 h and 48 h) was determined using Student's *t*-test (*$p < 0.05$, **$p < 0.01$). Data represent the means ± SDs ($n = 4$ devices).

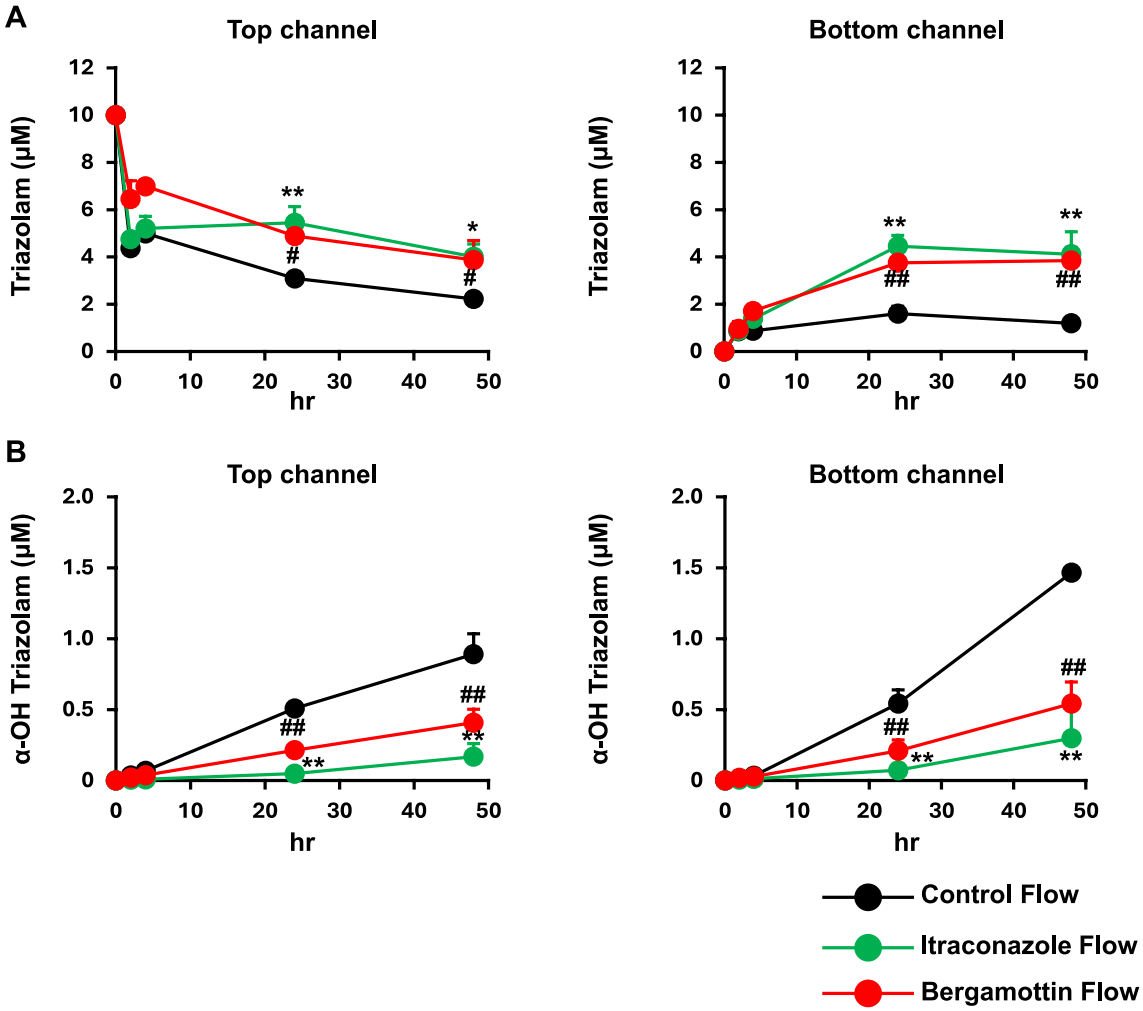

Fig. 5. The genome-edited chip can be utilized to analyze drug–drug and drug–food interactions. To inhibit CYP3A4 activity, the top channel of the genome-edited chips was treated with 10 μM itraconazole or 10 μM bergamottin for 24 h. (**A**) Apical-to-basolateral permeability of 10 μM triazolam in the genome-edited chip. (**B**) CYP3A4 activities in the genome-edited chip were examined by quantifying the metabolites of α-OH triazolam. Statistical significance was evaluated by one-way ANOVA followed by Dunnett's post hoc test [$^{*}p < 0.05$, $^{**}p < 0.01$: compared with the same time points (24 h and 48 h) between the Control Flow and Itraconazole-treated Flow, $\#p < 0.05$, $\#\#p < 0.01$: compared with the same time points (24 h and 48 h) between the Control Flow and Bergamottin-treated Flow. Data represent the means ± SDs ($n = 3$ devices).

under the flow conditions (Fig. 4D). While the ISOPRO concentration in the bottom channel increased under flow conditions, no change was observed in the top channel (Fig. 4D).

These results indicate that the genome-edited chip can effectively evaluate both drug absorption and metabolism simultaneously.

Genome-edited chip can be utilized to assess drug–drug and drug–food interactions

To determine whether the genome-edited chip can be used to evaluate drug–drug and drug–food interactions, we conducted experiments using itraconazole, an antifungal drug that inhibits CYP3A4, and bergamottin, a compound in grapefruit juice that also inhibits CYP3A4. Itraconazole or bergamottin was applied only to the top channel 24 h prior to the start of the experiment. Under flow conditions, administration of itraconazole or bergamottin resulted in increased triazolam concentrations in both the top and bottom channels at 24 and 48 h (Fig. 5A). Consistent with the increase in triazolam concentrations due to CYP3A4 inhibitor, α-OH triazolam concentrations decreased in both the top and bottom channels at 24 and 48 h after administration of itraconazole or bergamottin (Fig. 5B). These results suggest that the genome-edited chip can be used to evaluate drug–drug and drug–food interactions caused by CYP3A4 inhibition.

Discussion

The co-culture of Caco-2 and HepG2 cells on the PDMS device did not result in a significant increase in the gene expression levels of drug-metabolizing enzymes (Fig. 1B,C). However, since both cell types can be readily

cultured in medium containing 10% FBS, there is no need to adjust medium conditions during co-culture, which presents a major advantage. On the other hand, human iPS cell-derived intestinal epithelial-like and hepatocyte-like cells, as well as human small intestinal and liver organoids, are promising new cell resources for use in microfluidic devices[27–29]. However, these cells require media with complex compositions, making it challenging to establish co-culture conditions that preserve their functionality. Indeed, in the MPS co-culturing human iPSC (induced pluripotent stem cell)-derived intestinal epithelial-like cells and PXB-cells®, a significant issue has been reported: depending on the culture medium conditions, there can be a marked increase in *ALB* expression levels in the iPSC-derived intestinal epithelial-like cells[19]. These findings suggest that, while using cell lines such as Caco-2 and HepG2 cells in MPS is operationally straightforward, their co-culture is not likely to enhance drug metabolism capacity. Therefore, selecting appropriate cells and optimizing the culture conditions will be critical challenges in advancing MPS development.

The genome-edited chip under flow conditions showed higher metabolite concentrations for CYP1A2, CYP2C9, CYP2D6, and CYP3A4 in both the top and bottom channels compared to the WT chip under flow conditions (Fig. 4). The cells of the WT chip exhibited a low capacity for drug metabolism and thus were not suitable for use in analyzing drug metabolism. These results demonstrate that genome-edited Caco-2 cells and CYPs-UGT1A1 KI-HepG2 cells maintain high drug-metabolizing capacity even on the PDMS device. This finding suggests the utility of the MPS using cells overexpressing target genes. For example, it is predicted that cells overexpressing drug transporters will similarly maintain their function. Therefore, an MPS incorporating cells overexpressing specific genes, tailored to the experimental purpose, is likely to be a straightforward and cost-effective model. This approach has the potential to be widely applied as an efficient and reliable in vitro evaluation system for pharmacokinetic studies and toxicity assessments.

Compared to static conditions, under flow conditions, the amount of parent compound permeating into the bottom channel and the amount of metabolites increased (Figs. 3, 4). Previous studies have reported improvements in cell function when cells are seeded onto MPS under dynamic perfusion conditions[30–32]. In this study, experiments were conducted under conditions where dynamic perfusion was applied only during drug absorption and metabolism experiments. Therefore, we speculate that the increase in the amount of parent compound permeating into the bottom channel and metabolites was due to the perfusion of stagnant medium rather than an improvement in cell function. Interestingly, the concentration of 4-OH diclofenac in the genome-edited chip flow top channel was lower than that in the genome-edited chip static top channel (Fig. 4B). 4-OH diclofenac is the major metabolite of diclofenac, but other metabolites, such as 5-OH diclofenac and those conjugated by UGT, also exist[33–35]. Therefore, dynamic perfusion may have led to the drug metabolite production, resulting in increased production of 4-OH diclofenac conjugates and other metabolites.

Under static conditions, the concentrations of APAP and caffeine in the top channel remained nearly unchanged from the initial concentration, but the amount of drug permeating into the bottom channel increased over time (Fig. 3A,B). Theoretically, an increase in drug penetration into the bottom channel should lead to a decrease in concentration in the top channel. In this experiment, drug absorption and metabolism experiments were conducted with 300 µL of liquid in the top channel and 200 µL in the bottom channel. We speculate that the difference in liquid volume may have prevented changes in drug concentration in the top channel.

According to the package insert for triazolam, coadministration with itraconazole is contraindicated, while caution is advised when co-administering grapefruit juice. It is well established that both itraconazole and grapefruit juice increase the area under the curve (AUC) of triazolam[36,37]. In the present study, treatment with either itraconazole or bergamottin led to increased triazolam concentrations and decreased α-OH triazolam concentrations in both the top and bottom channels of the genome-edited chip under flow conditions, consistent with clinical observations. However, it should be noted that grapefruit juice contains components other than bergamottin that can also inhibit CYP3A4[38,39].

In this study, the metabolism of propranolol was assessed using ISOPRO, a CYP1A2 metabolite, as an indicator (Fig. 4D). The major metabolite of propranolol, 4-hydroxy propranolol (4-OH propranolol), which is produced by CYP2D6[40,41], is extremely unstable and could not be measured in medium containing 10% FBS. Our previous studies demonstrated that 4-OH propranolol metabolism can be effectively assessed by culturing CYPs-UGT1A1 KI-HepG2 cells in HBSS[14]. Consistent with these findings, the concentration of propranolol in the bottom channel of the genome-edited chip under flow conditions peaked at 4 h, and then declined, and finally became lower compared to that in the WT chip under flow conditions. This decrease may reflect the metabolic activity of both CYP2D6 and CYP1A2. Similarly, the concentration of ISOPRO in the bottom channel of the genome-edited chip under flow conditions also peaked at 24 h and then decreased (Fig. 4D). ISOPRO is known to undergo glucuronidation and sulfate conjugation[42], and therefore the decrease was likely due to these phase II conjugation reactions mediated by drug-metabolizing enzymes such as UGT.

Several studies have reported the fabrication of intestinal chips with villus-like structures by incorporating Caco-2 cells, human iPS cell-derived intestinal epithelial-like cells or human intestinal organoids into MPS[28,43,44]. In this study, however, the Caco-2 cells used in our intestine-liver-on-a-chip were cultured as a conventional monolayer. If drug absorption experiments could be conducted using a model with villus structures, it may be possible to predict intestinal absorption (*Fa*, fraction absorbed) with higher accuracy compared to the monolayer model. Nevertheless, to the best of our knowledge, there have been no reports that have directly compared *Fa* between villus-structured and monolayer in vitro models using several drugs with varying intestinal absorption characteristics. It is therefore necessary to first evaluate the differences in absorption rates between these two types of models. In our intestine-liver-on-a-chip, the HepG2 cells were not cultured to confluency. If CYPs-UGT1A1 KI-HepG2 cells could be used under confluent conditions, a higher level of drug metabolites could likely be detected. Unfortunately, when the HepG2 cells were seeded to reach confluency in the bottom channel of the PDMS device, clogging of the microchannel occurred. As a result, the number of HepG2 cells that can

be seeded in the bottom channel is limited. Similarly, clogging may also occur in intestinal chips with villus structures, indicating that improvements in the PDMS device design are necessary.

In addition to the present study, several MPS models incorporating both intestinal epithelial cells and hepatocytes for pharmacokinetic studies have been reported[19,45]. Arakawa et al. demonstrated that an MPS incorporating Caco-2 and HepaRG cells could predict the pharmacokinetics of triazolam; however, their evaluation was limited to triazolam alone[18]. Sakai et al. reported an MPS incorporating human iPS cell-derived intestinal epithelial-like cells and PHHs, but their assessment was limited to transepithelial electrical resistance (TEER) measurements and gene expression levels of cytochrome P450[46]. Similarly, in studies utilizing MPS models incorporating Caco-2 and HepG2 cells, evaluations have been limited to the metabolism of phenacetin to acetaminophen[47]. In contrast, our study conducted absorption and metabolism experiments focusing on major cytochrome P450, evaluating not only the concentrations of metabolites but also those of the parent compounds. These findings are expected to provide valuable insights for the future development of intestine-liver-on-a-chip chips intended for pharmacokinetic testing.

Limitations

This study was initiated with the goal of predicting first-pass effects. Depending on the drug administered orally, the drug generally becomes systemic available within about 30 min to several hours after administration. However, our experiments using the intestine-liver-on-a-chip assessed the system up to 48 h. With a culture surface area of 0.22 cm^2, the intestine-liver-on-a-chip makes it challenging to evaluate drug metabolism over short periods. Future efforts to increase the culture surface area of PDMS devices and to develop mathematical models that incorporate scale factors and other relevant parameters would be beneficial. The intestine-liver-on-a-chip used in this study was cultured and tested under static and flow conditions. It should be noted that the use of the Infinity Rocker Pro to reproduce flow conditions generates bidirectional flow, which lacks important characteristics of physiological perfusion, including unidirectionality, continuous flow, and precise shear stress control. Therefore, future validation studies using pump-based systems that achieve unidirectional and continuous flow are necessary.

Although PDMS devices were used in this study, it is known that PDMS tends to sorb highly lipid-soluble drugs[23,25,26]. In this study as well, triazolam, bufuralol, and propranolol were substantially adsorbed onto the PDMS device within 2 h. Therefore, it is difficult to accurately determine whether the reduction in parent compound concentration is due to drug adsorption onto PDMS or drug metabolism. Calculating the drug adsorption rate onto PDMS and correcting drug concentrations based on this rate is considered effective. However, correcting metabolite quantities when parent compounds have adsorbed onto PDMS and parent compound concentrations have decreased is challenging. Consequently, drug metabolism experiments on PDMS devices may underestimate the extent of drug metabolism, as drugs that are easily metabolized by CYPs are often highly lipophilic. Therefore, when PDMS devices are employed, it remains crucial to evaluate in advance whether the drug will be adsorbed.

Recent efforts have focused on developing microfluidic device materials with lower drug sorption or using PDMS-PEG block copolymers as alternatives to PDMS[48–51]. We believe that it is more important to develop MPS devices using materials with low drug adsorption rates than to correct the drug adsorption rate to PDMS. However, even in devices using materials with low drug adsorption properties, the adsorption of bufuralol used in this study was significant and has not been completely resolved[52]. On the other hand, rigid plastic materials such as polystyrene pose minimal issues with drug adsorption and are widely used in drug absorption and metabolism experiments. Mimetas, for example, markets the OrganoPlate®[53], a device based on such rigid plastic materials. Given these advantages, device development utilizing rigid plastic materials is considered important, in addition to silicone-based materials like PDMS.

Conclusion

A genome-edited chip was generated by loading high-drug-metabolism capacity genome-edited Caco-2 cells and CYPs-UGT1A1 KI-HepG2 cells onto a PDMS device. This study demonstrated that the genome-edited chip can be used simply and cost-effectively for drug absorption and metabolism experiments that consider the effects of the small intestine and liver. Furthermore, the genome-edited chip is also applicable to CYP3A4 inhibition experiments, suggesting its usefulness for evaluating drug–drug interactions and drug–food interactions.

Data availability

The authors declare that all the data related to this study are available within the paper or can be obtained from the corresponding author upon reasonable request.

Received: 19 December 2024; Accepted: 29 September 2025
Published online: 04 November 2025

References

1. Sun, H., Chow, E. C., Liu, S., Du, Y. & Pang, K. S. The Caco-2 cell monolayer: usefulness and limitations. *Expert Opin. Drug Metab. Toxicol.* **4**, 395–411 (2008).
2. Balimane, P. V. & Chong, S. Cell culture-based models for intestinal permeability: a critique. *Drug Discov. Today* **10**, 335–343 (2005).
3. Watanabe, K., Negoro, R. & Fujita, T. 5-ALA treatment increases intracellular heme levels and enhances CYP3A4 activity in genome-edited Caco-2 cells. *Biochem. Biophys. Res. Commun.* **664**, 94–99 (2023).
4. Negoro, R., Yamada, N., Watanabe, K., Kono, Y. & Fujita, T. Generation of Caco-2 cells stably expressing CYP3A4·POR·UGT1A1 and CYP3A4·POR·UGT1A1*6 using a PITCh system. *Arch. Toxicol.* **96**, 499–510 (2022).

5. Li, A. P. et al. Cryopreserved human hepatocytes: characterization of drug-metabolizing enzyme activities and applications in higher throughput screening assays for hepatotoxicity, metabolic stability, and drug-drug interaction potential. *Chem. Biol. Interact.* **121**, 17–35 (1999).
6. Brandon, E. F. A., Raap, C. D., Meijerman, I., Beijnen, J. H. & Schellens, J. H. M. An update on in vitro test methods in human hepatic drug biotransformation research: pros and cons. *Toxicol. Appl. Pharmacol.* **189**, 233–246 (2003).
7. Arzumanian, V. A., Kiseleva, O. I. & Poverennaya, E. V. The curious case of the HepG2 cell line: 40 years of expertise. *Int. J. Mol. Sci.* **22**, 13135 (2021).
8. Hart, S. N. et al. A comparison of whole genome gene expression profiles of HepaRG cells and HepG2 cells to primary human hepatocytes and human liver tissues. *Drug Metab. Dispos.* **38**, 988–994 (2010).
9. Musther, H., Olivares-Morales, A., Hatley, O. J. D., Liu, B. & Rostami Hodjegan, A. Animal versus human oral drug bioavailability: Do they correlate?. *Eur. J. Pharm. Sci.* **57**, 280–291 (2014).
10. Akabane, T. et al. A comparison of pharmacokinetics between humans and monkeys. *Drug Metab. Disposit.* **38**, 308–216 (2010).
11. Naritomi, Y., Sanoh, S. & Ohta, S. Chimeric mice with humanized liver: Application in drug metabolism and pharmacokinetics studies for drug discovery. *Drug Metab. Pharmacokinet.* https://doi.org/10.1016/j.dmpk.2017.11.001 (2018).
12. Scheer, N. & Wilson, I. D. A comparison between genetically humanized and chimeric liver humanized mouse models for studies in drug metabolism and toxicity. *Drug Discov. Today* **21**, 250–263 (2016).
13. Yamada, N., Negoro, R., Watanabe, K. & Fujita, T. Generation of Caco-2 cells with predictable metabolism by CYP3A4, UGT1A1 and CES using the PITCh system. *Drug Metab. Pharmacokinet.* **50**, 100497 (2023).
14. Negoro, R., Tasaka, M., Deguchi, S., Takayama, K. & Fujita, T. Generation of HepG2 cells with high expression of multiple drug-metabolizing enzymes for drug discovery research using a PITCh system. *Cells* **11**, 1677 (2022).
15. Negoro, R., Ouchi, A., Deguchi, S., Takayama, K. & Fujita, T. Refining hepatocyte models to capture the impact of CYP2D6*10 utilizing a PITCh system. *Biol. Pharm. Bull.* **47**, 1422–1428 (2024).
16. Huh, D., Hamilton, G. A. & Ingber, D. E. From 3D cell culture to organs-on-chips. *Trends Cell Biol.* **21**, 745–754 (2011).
17. Vulto, P. & Joore, J. Adoption of organ-on-chip platforms by the pharmaceutical industry. *Nat. Rev. Drug Discov.* **20**, 961–962. https://doi.org/10.1038/s41573-021-00323-0 (2021).
18. Arakawa, H. et al. Kinetic analysis of sequential metabolism of triazolam and its extrapolation to humans using an entero-hepatic two-organ microphysiological system. *Lab Chip* **20**, 537–547 (2020).
19. Shinohara, M. et al. Coculture with hiPS-derived intestinal cells enhanced human hepatocyte functions in a pneumatic-pressure-driven two-organ microphysiological system. *Sci. Rep.* **11**, 5437 (2021).
20. Milani, N. et al. Application of a gut-liver-on-a-chip device and mechanistic modelling to the quantitative in vitro pharmacokinetic study of mycophenolate mofetil. *Lab Chip* **22**, 2853–2868 (2022).
21. Yang, J. et al. Gut-liver-axis microphysiological system for studying cellular fluidic shear stress and inter-tissue interaction. *Biomicrofluidics* **16**, 044113 (2022).
22. Herland, A. et al. Quantitative prediction of human pharmacokinetic responses to drugs via fluidically coupled vascularized organ chips. *Nat. Biomed. Eng.* **4**, 421–436 (2020).
23. Deguchi, S. et al. Usability of polydimethylsiloxane-based microfluidic devices in pharmaceutical research using human hepatocytes. *ACS Biomater. Sci. Eng.* **7**, 3648–3657 (2021).
24. Varma, M. V. S. et al. Physicochemical space for optimum oral bioavailability: Contribution of human intestinal absorption and first-pass elimination. *J. Med. Chem.* **53**, 1098–1108 (2010).
25. Carius, P. et al. Addressing the ADME Challenges of compound loss in a PDMS-based gut-on-chip microphysiological system. *Pharmaceutics* **16**, 296 (2024).
26. Grant, J. et al. Simulating drug concentrations in PDMS microfluidic organ chips. *Lab Chip* **21**, 2509–3519 (2021).
27. Shin, W., Hinojosa, C. D., Ingber, D. E. & Kim, H. J. Human intestinal morphogenesis controlled by transepithelial morphogen gradient and flow-dependent physical cues in a microengineered gut-on-a-chip. *iScience* **15**, 391–406 (2019).
28. Deguchi, S. et al. Construction of multilayered small intestine-like tissue by reproducing interstitial flow. *Cell Stem Cell* **31**, 1315-1326.e8 (2024).
29. Wang, Y., Wang, H., Deng, P., Chen, W. & Guo, Y. In situ differentiation and generation of functional liver organoids from human iPSCs in a 3D perfusable chip system. *Lab Chip* https://doi.org/10.1039/c8lc00869h (2018).
30. Rahman, S. M. et al. Opportunities and challenges for human microphysiological systems in drug development. *ALTEX-Alternat. Animal Experiment.* **42**, 224–256 (2025).
31. Petit, I. et al. Proximal tubule-on-chip as a model for predicting cation transport and drug transporter dynamics. *Sci. Rep.* **15**, 2580 (2025).
32. Intestine, H. et al. Microfluidic organ-on-a-chip models of human intestine. *Cell Mol. Gastroenterol. Hepatol.* **5**, 659–668 (2018).
33. Ahire, D., Heyward, S. & Prasad, B. Intestinal metabolism of diclofenac by polymorphic UGT2B17 correlates with its highly variable pharmacokinetics and safety across populations. *Clin. Pharmacol. Ther.* **114**, 161–172 (2023).
34. Bort, R. et al. Hepatic metabolism of diclofenac: Role of human CYP in the minor oxidative pathways. *Biochem. Pharmacol.* **58**, 787–796 (1999).
35. Lazarska, K. E., Dekker, S. J., Vermeulen, N. P. E. & Commandeur, J. N. M. Effect of UGT2B7*2 and CYP2C8*4 polymorphisms on diclofenac metabolism. *Toxicol. Lett.* **284**, 70–78 (2018).
36. Hukkinen, S. K., Varhe, A., Olkkola, K. T. & Neuvonen, P. J. Plasma concentrations of triazolam are increased by concomitant ingestion of grapefruit juice. *Clin. Pharmacol. Ther.* **58**, 127–131 (1995).
37. Varhe, A., Olkkola, K. T. & Neuvonen, P. J. Oral triazolam is potentially hazardous to patients receiving systemic antimycotics ketoconazole or itraconazole. *Clin. Pharmacol. Ther.* **56**, 601–607 (1994).
38. Kakar, S. M., Paine, M. F., Stewart, P. W. & Watkins, P. B. 6′7′-dihydroxybergamottin contributes to the grapefruit juice effect. *Clin. Pharmacol. Ther.* **75**, 569–579 (2004).
39. Guo, L. Q., Fukuda, K., Ohta, T. & Yamazoe, Y. Role of furanocoumarin derivatives on grapefruit juice-mediated inhibition of human CYP3A activity. *Drug Metab. Dispos.* **28**, 766–771 (2000).
40. Otey, C. R., Bandara, G., Lalonde, J., Takahashi, K. & Arnold, F. H. Preparation of human metabolites of propranolol using laboratory-evolved bacterial cytochromes P450. *Biotechnol. Bioeng.* **93**, 494–499 (2006).
41. Upthagrove, A. L. & Nelson, W. L. Importance of amine pKa and distribution coefficient in the metabolism of fluorinated propranolol derivatives. Preparation, identification of metabolite regioisomers, and metabolism by CYP2D6. *Drug Metab. Dispos.* **29**, 1377–1388 (2001).
42. Walle, T., Walle, U. K. & Olanoff, L. S. Quantitative account of propranolol metabolism in urine of normal man. *Drug Metab. Dispos.* **13**, 204–209 (1985).
43. Kasendra, M. et al. Development of a primary human Small Intestine-on-a-Chip using biopsy-derived organoids. *Sci. Rep.* **8**, 2871 (2018).
44. Shin, W. & Kim, H. J. Intestinal barrier dysfunction orchestrates the onset of inflammatory host–microbiome cross-talk in a human gut inflammation-on-a-chip. *Proc. Natl. Acad. Sci.* **115**, E10539–E10547 (2018).
45. Hu, W. et al. Microfluidic organ-on-a-chip models for the gut–liver axis: from structural mimicry to functional insights. *Biomater. Sci.* **13**, 1624–1656 (2025).
46. Sakai, Y. et al. Development of a perfusing small intestine-liver microphysiological system device. *Appl. Sci. (Switzerland)* **13**, 10510 (2023).

47. Bricks, T. et al. Development of a new microfluidic platform integrating co-cultures of intestinal and liver cell lines. *Toxicol. Vitro* **28**, 885–895 (2014).
48. Wang, M. et al. Perfluoropolyether-based gut-liver-on-a-chip for the evaluation of first-pass metabolism and oral bioavailability of drugs. *Cite This: ACS Biomater. Sci. Eng.* **10**, 4635–4644 (2024).
49. Sano, E. et al. Generation of tetrafluoroethylene-propylene elastomer-based microfluidic devices for drug toxicity and metabolism studies. *ACS Omega* **6**, 24859–24865 (2021).
50. Mair, D. B. et al. PDMS-PEG block copolymer and pretreatment for arresting drug absorption in microphysiological devices. *ACS Appl. Mater. Interfaces* **14**, 38541–24548 (2022).
51. Ueno, R. et al. Relationship between adsorption and toxicity of nephrotoxic drugs in microphysiological systems (MPS). *Micromachines (Basel)* **14**, 761 (2023).
52. Wang, M. et al. Application of perfluoropolyether elastomers in microfluidic drug metabolism assays. *Int. J. Pharm.* **627**, 122253 (2022).
53. Nicolas, A. et al. High throughput transepithelial electrical resistance (TEER) measurements on perfused membrane-free epithelia. *Lab Chip* **21**, 1676–1685 (2021).

Acknowledgements

This research was supported by Japan Agency for Medical Research and Development (AMED) (Grant Number JP22mk0101214) and The Nakatani Foundation for Advancement of Measuring Technologies in Biomedical Engineering. We thank Ms. Kaori Kosugi (Kyoto University) for fabricating PDMS device.

Author contributions

R.N., Research design, Methodology, Conducted experiments, Data analyses, Funding acquisition, Writing paper, Final approval S.D., Methodology, Preparing PDMS devices D.Y., Discussion K.T., Methodology, Preparing PDMS devices T.F., Discussion.

Declarations

Competing interests

The authors declare no competing interests.

Declaration of generative AI and AI-assisted technologies in the writing process

While writing this manuscript, the authors used DeepL, Grammarly, ChatGPT, and Claude to improve the grammatical accuracy and readability of the English. After using these tools, they carefully reviewed and edited the content as needed and are fully responsible for the publication content.

Additional information

Supplementary Information The online version contains supplementary material available at https://doi.org/10.1038/s41598-025-22425-0.

Correspondence and requests for materials should be addressed to R.N.